The Effect of Biaxial Orientation and Crystallinity on the Long-Term Creep Behavior of Poly(ethylene Terephthalate) Films below Glass Transition Temperature

M. CAKMAK* and Y. D. WANG† *Institute of Polymer Engineering, University of Akron, Akron, Ohio 44325*

Synopsis

The use of thin polymeric films in applications such as flexible circuit boards and dish membrane solar collectors has been gaining popularity. In these and many other applications the films are used under constant loading conditions which subjects them to long-term creep. In this paper, we present detailed experimental tensile creep results on unoriented films of varying crystallinities and unequal and equal biaxially oriented poly(ethylene terephthalate) (PET) films. The results indicate that the increase of crystallinity, stretch ratios, and annealing causes reduction in long-term creep strains. Unequal biaxially stretched films exhibited in-plane anisotropy in their tensile creep behavior. In these films the lowest creep strains are observed in the direction along which the film stretched to the highest stretch ratio.

INTRODUCTION

Long-term creep behavior of materials has been of concern to engineers designing products used under constant load. Early studies in this area were primarily concentrated on metals and in the past 30 years research activities on polymers has been intensified. The majority of creep studies were on unoriented glassy polymers such as PMMA,[1,2] PVC,[3,4] CAB (cellulose acetate buthyrate),[5] and on unoriented semicrystalline polymers including polyethylene,[4,6-8] polypropylene,[3,6,10,11] filled polypropylene[12] and crystalline poly(ethylene terephthalate).[13] There has been very limited study on the effect of crystallinity and chain orientation on the creep behavior of these materials. Some of these studies are on uniaxially stretched PP,[14,15] uniaxially stretched PE,[16] ultradrawn PE[20] and a biaxially stretched PET film.[21] There are also some studies on the effect of radiation on creep behavior of PE,[22] PP,[23] and drawn PP.[24]

To our knowledge, no thorough study on the effect of crystallinity, type and level of orientation on the long-term creep behavior of biaxially oriented films have been reported. In this study, we are primarily concerned with the effect of crystallinity and biaxial stretching conditions on the long-term creep behavior of PET films.

* To whom all correspondence should be addressed.

† Present address: Shenyang Research Institute of Plastics, Shenyang, P. R. of China.

Journal of Applied Polymer Science, Vol. 41, 1867–1890 (1990)
 CCC 0021-8995/90/7-81867-24$04.00

EXPERIMENTAL

Materials and Processing

Initially amorphous and unoriented melt cast films of PET were supplied by Tennessee Eastman Company (Tenite 7352). Initial thickness of these films was 546 μm.

Biaxial Stretching

Biaxial stretching of PET films were performed using an Iwamoto Seisakusho (Model BIX-702) biaxial stretcher. As-received cast PET films were cut to 14 $\times$ 14 cm square samples which were then placed in the preheated biaxial stretcher and clamped around the edges with pneumatic clamps. Actual gauge distance between the clamps was kept at 12 cm. After 7 min of temperature equilibration, the samples were stretched biaxially simultaneously to desired stretch ratios in both axes. After the completion of stretching, the samples were cooled down to 65°C and removed from the clamps. Three series of films were stretched at 80, 90, and 100°C at 1, 5, 10, and 20 mm/s stretching speeds in simultaneous biaxial stretching mode.

Annealing

To investigate the effect of crystallinity on tensile creep behavior of PET films, a series of samples were prepared by annealing the cast amorphous PET films in a forced draft oven at 170°C for times ranging from 1 to 720 min. These samples were clamped on an adjustable square sandwich frame during annealing. This frame was also used for annealing stretched PET films (3 $\times$ 3) to prevent shrinkage in the plane of the film. For these oriented PET films the annealing temperature was kept at 150°C and the annealing time was varied from 5 to 30 min.

Differential Scanning Calorimetry

Thermal properties of selected films were characterized using a Dupont DSC 9900 apparatus. The DSC scan rate was kept constant at 20°C/min. The crystallinities of PET films were determined by subtracting the area under the cold crystallization peak from the melting peak ($\Delta H_{exp} = \Delta H_m - \Delta H_c$) then crystallinities were calculated using the following equation

$$X(\%) = \frac{\Delta H_{exp}}{\Delta H^0} \tag{1}$$

where ΔH^0 is the heat of fusion of 100% crystalline polymer. The value for PET is 126.4 J/g.[25]

The annealed PET samples showed two melting peaks (endotherms) in their DSC scans. The crystallinities for these samples were calculated using the ΔH_{exp} obtained by adding the area under the two peaks. The location of main transitions were obtained with the Dupont Data Analysis Software.

Optical Properties

Principal refractive indices of oriented PET films were measured using a polarized Abbe refractometer technique described elsewhere.[26,27] Methylene iodide was used as an immersion liquid. A sodium illumination source was used to improve the accuracy of measurements.

Creep Measurements

Tensile creep and recovery measurements were performed using a dead-load apparatus designed and built in our laboratories for testing 7 thin polymer films simultaneously. This multistation creep testing assembly is enclosed with an environmental chamber in which the temperature is controlled within ± 1.5°C of the set point. As shown schematically in Figure 1, the sample is clamped by upper and lower grips and the lower grip was connected with a dial gauge using a piano wire which has very low elastic deflection. The strains of the specimens were calculated by grip displacements that were measured by the dial gauges. In a separate experiment, each creep station was loaded with a microtome blade and the elastic deflection of each station was recorded as a function of load. The final creep data for PET films were corrected using the above calibration curves for each station.

Strips with 9 × 0.5–1 cm dimensions were cut from the selected films with their long axes along the desired direction. To begin the creep test, the samples

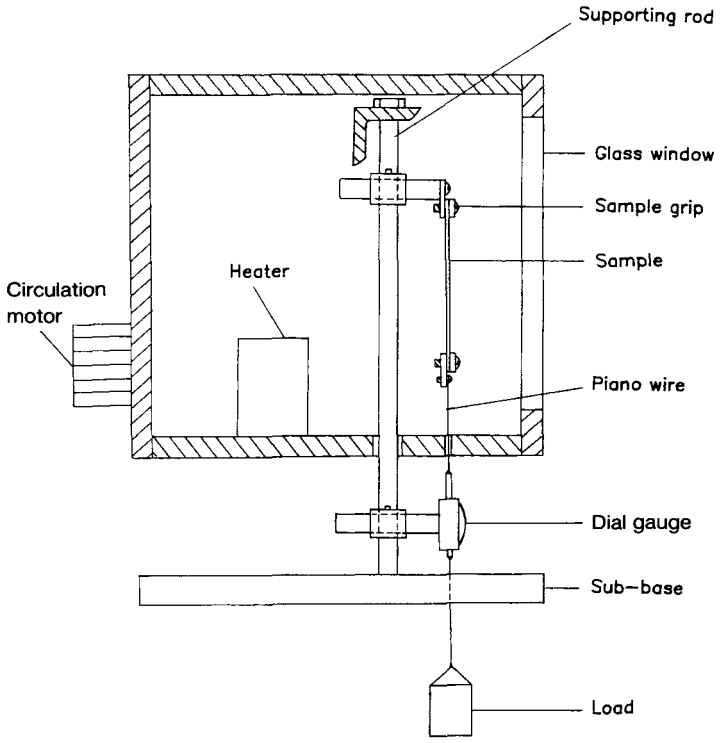

Fig. 1. Creep testing assembly.

were conditioned at the set temperature for 1.5 h before the load was applied. The samples were load conditioned[17,20] by first smoothly applying the load under which they are to be tested. This load was removed after 10 sec and sample was maintained under this condition for additional 100 sec. This procedure was repeated at least three times until the readings obtained on the dial gauge upon removal of the load became repeatable. The samples were then loaded to desired stress level for the last time and this marked the beginning of the creep experiment. The data were recorded at regular time intervals from the dial gauges. The accuracy of the data was limited by the resolution of the dial gauges ($\pm$ 0.0005 in., $\pm$ 0.0127 mm).

To test the effect of sample gauge length on creep response, unstretched PET sample was load conditioned and loaded to 13.78 MPa (2000 psi) stress level and after 20 min the displacement was recorded. Then the load was removed and the sample was allowed to recover. It was again reconditioned and reloaded. This measurement was repeated 5 times for several different gauge lengths. The mean strain value measured after 20 min as a function of the sample gauge length is plotted in Figure 2. This figure indicates that the shorter the sample gauge length, the higher the relative deviation of measurements and also the larger the strain measured because of the additional extension near the grips. It can be seen that for the samples which have gauge lengths longer than 6 cm there is no appreciable effect. In all the data presented in this study, the gauge length was kept to 6 cm in order to avoid larger measurement deviation.

Table I lists all the samples and creep test conditions investigated.

RESULTS AND DISCUSSIONS

Crystallinity Development in Processed Films

Unoriented Films

Crystallinities of unoriented annealed films are shown in Figure 3. As received cast films exhibit about 7% crystallinity and with the increase of annealing

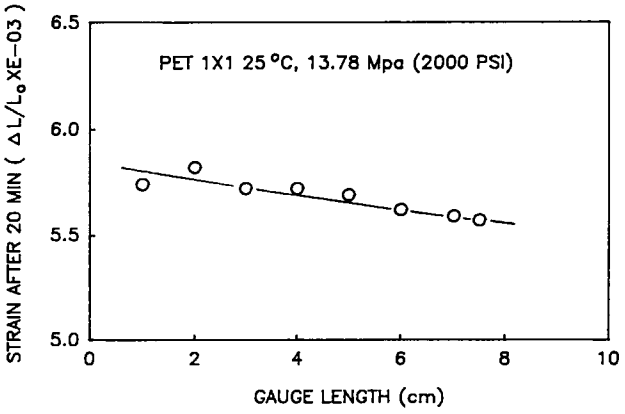

Fig. 2. Effect of gauge length on the creep strains.

TABLE I
Sample Processing and Testing Conditions

Stretching condition			Creep test condition		
Stretch ratio	Temperature (°C)	Speed (mm/sec)	Temperature (°C)	Stress	Period (h)
1 × 1	Unstretched		30	6.89 MPa (1000 psi)	380
1 × 1	Unstretched		30	13.78 MPa (2000 psi)	380
2 × 2	80	10	30	6.89 MPa (1000 psi)	380
2 × 2	80	10	30	13.78 MPa (2000 psi)	380
3 × 3	80	10	30	6.89 MPa (1000 psi)	380
3 × 3	80	10	30	13.78 MPa (2000 psi)	380
1 × 1	Unstretched		40	13.78 MPa (2000 psi)	300
2 × 2	80	10	40	13.78 MPa (2000 psi)	300
2 × 2	90	10	40	13.78 MPa (2000 psi)	300
2 × 2	100	10	40	13.78 MPa (2000 psi)	300
3 × 3	80	10	40	13.78 MPa (2000 psi)	300
3 × 3	90	10	40	13.78 MPa (2000 psi)	300
3 × 3	100	10	40	13.78 MPa (2000 psi)	300
1 × 1	Unstretched		50	13.78 MPa (2000 psi)	300
2 × 2	80	10	50	13.78 MPa (2000 psi)	300
3 × 1	80	10	50	13.78 MPa (2000 psi)	300
3 × 2	80	10	50	13.78 MPa (2000 psi)	300
3 × 3	80	1	50	13.78 MPa (2000 psi)	300
3 × 3	80	5	50	13.78 MPa (2000 psi)	300
3 × 3	80	10	50	13.78 MPa (2000 psi)	300
3 × 3	80	20	50	13.78 MPa (2000 psi)	300
3 × 3	90	10	50	13.78 MPa (2000 psi)	300
3 × 3	100	10	50	13.78 MPa (2000 psi)	300
2 × 2	80	10	50	20.67 MPa (3000 psi)	300
3 × 3	80	10	50	20.67 MPa (3000 psi)	300
Annealed PET					
3 × 3 (5 min)	80	10	50	13.78 MPa (2000 psi)	300
3 × 3 (10 min)	80	10	50	13.78 MPa (2000 psi)	300
3 × 3 (30 min)	80	10	50	13.78 MPa (2000 psi)	300
1 × 1 (1 min)	Unstretched		50	13.78 MPa (2000 psi)	300
1 × 1 (2 min)	Unstretched		50	13.78 MPa (2000 psi)	300
1 × 1 (12 h)	Unstretched		50	13.78 MPa (2000 psi)	300

time at 170°C, annealing temperature crystallinities increase to about 40% monotonously with tendency to level off at long annealing times.

Oriented Films

As shown in Figure 4 biaxial stretching at 80°C increases the crystallinity of films up to 35%. This is the result of stress-induced crystallization typically occurring at this temperature.[27] Within the temperature range investigated, the increase of stretching temperature causes a reduction in crystallinity in films stretched to 2 × 2 stretch ratio (Fig. 5) indicating the increase of temperature reduces the effectiveness of stress on the crystallization or stress hardening threshold moves to higher stretch ratios. At 3 × 3 condition, on the other hand, this temperature effect is not observed and crystallinities obtained in

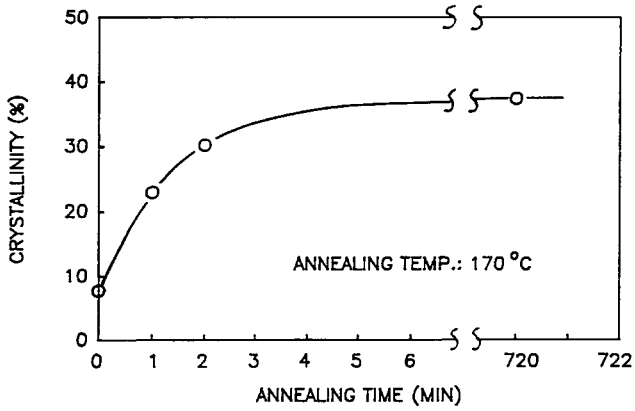

Fig. 3. Effect of annealing time on crystallinity of unoriented PET films (Temp: 170°C).

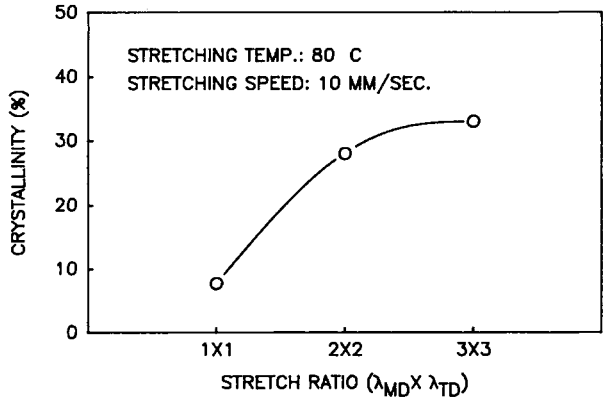

Fig. 4. Effect of equal biaxial stretching on crystallinity of PET films stretched at 80°C.

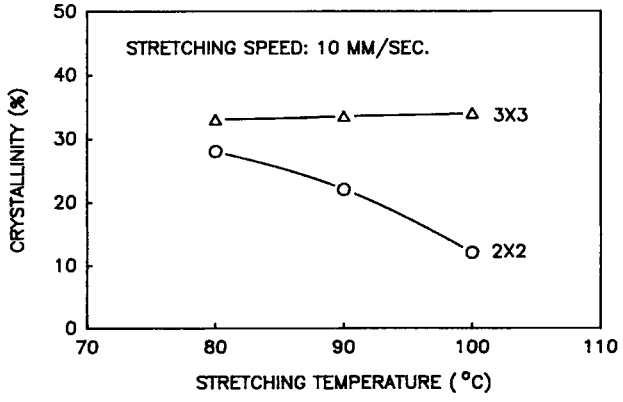

Fig. 5. Effect of stretching temperature on crystallinity of 2 × 2 and 3 × 3 stretched films.

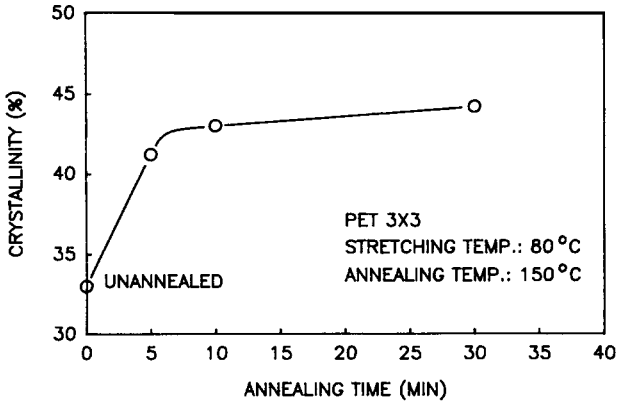

Fig. 6. Effect of annealing on crystallinity of 3 × 3 stretched PET films.

these films are unaffected by the stretching temperature. In all latter films, the onset of stress hardening point has been passed at the stretch ratio of 3 × 3 which is the reason for minimal differences in crystallinities of these films.

Annealing 3 × 3 stretched films at 150°C causes about 10% increase in crystallinity at a 30 min annealing time as shown in Figure 6.

Optical Properties

All refractive index data obtained on PET films are tabulated in Table II and birefringes calculated from these data are presented in Figures 7–11. Detailed analysis of these optical properties and their implications on the structure of the films is given elsewhere.[28]

TABLE II
Principal Refractive Indices of PET Films

Sample	n_{ND} (3)	n_{MD} (1)	n_{TD} (2)	Δn_{13}	Δn_{23}
Cast PET	1.5650	1.5667	1.5663	0.0017	0.0013
2 × 2 80°C 10 mm/s (1)	1.5507	1.5933	1.5909	0.0426	0.0402
2 × 2 80°C 10 mm/s (2)	1.5473	1.6017	1.6010	0.0544	0.0537
2 × 2 90°C 10 mm/s (1)	1.5509	1.6052	1.5977	0.0543	0.0468
2 × 2 90°C 10 mm/s (2)	1.5451	1.6103	1.6006	0.0652	0.0555
2 × 2 100°C 10 mm/s	1.5717	1.5800	1.5792	0.0083	0.0075
3 × 1 80°C 10 mm/s	1.5366	1.6491	1.5630	0.1125	0.0264
3 × 2 80°C 10 mm/s	1.5327	1.6290	1.5855	0.0963	0.0528
3 × 3 80°C 10 mm/s	1.5207	1.6217	1.6139	0.1010	0.0932
3 × 3 90°C 10 mm/s	1.5229	1.6230	1.6176	0.1001	0.0947
3 × 3 100°C 10 mm/s	1.5373	1.6151	1.6163	0.0778	0.0790
Annealed PET 3 × 3 10 mm/s					
5 min at 150°C	1.4994	1.6469	1.6428	0.1475	0.1434
10 min at 150°C	1.4998	1.6475	1.6445	0.1477	0.1447
30 min at 150°C	1.4991	1.6486	1.6466	0.1495	0.1475

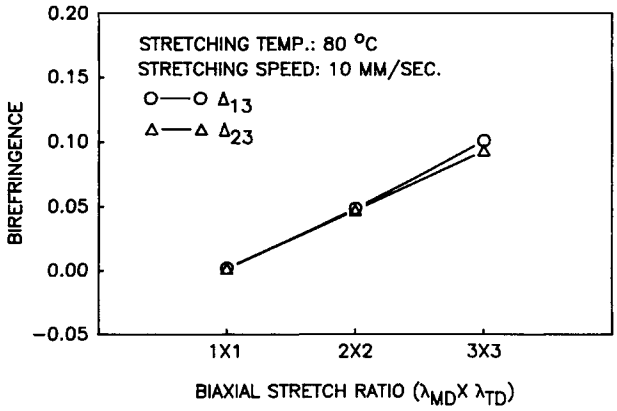

Fig. 7. Variation of Δn_{13} and Δn_{23} with biaxial stretch ratios (80°C unannealed).

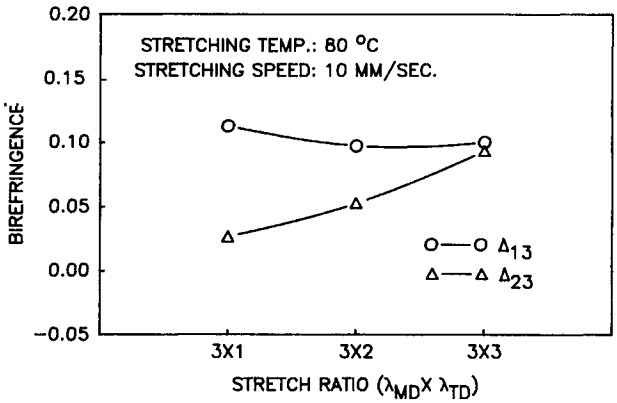

Fig. 8. Variation of Δn_{13} and Δn_{23} with λ_{TD} in films with constant $\lambda_{MD} = 3$ (80°C unannealed).

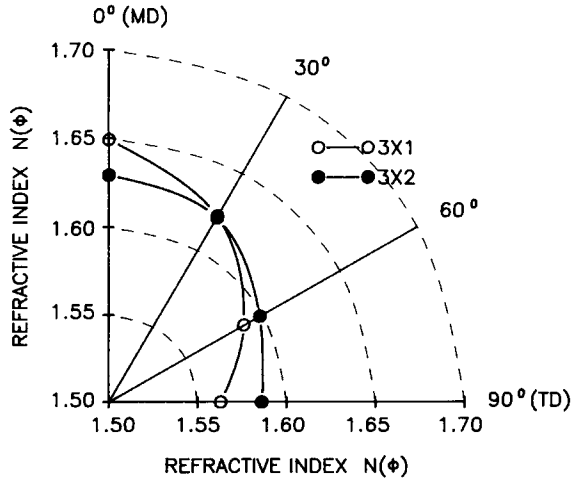

Fig. 9. In-plane anisotropy in 3 × 1 and 3 × 2 stretched films.

Both Δn_{13} and Δn_{23} increase monotonously with biaxial stretching (Fig. 7). Figure 8 show the effect of transverse direction stretching (increase of λ_{TD}) on Δn_{13} and Δn_{23}. In-plane variation of refractive indices of these films are also plotted in polar coordinates in Figure 9. The refractive index along TD increases and along MD decreases with the increase of stretch ratio in the transverse direction. Increase of stretching temperature causes a reduction in birefringences especially in films stretched to 2×2 stretch ratio (Figs. 10a and b). Note that similar reduction is observed in crystallinity values. Annealing 3×3 stretched films causes a rapid rise in Δn_{13} and Δn_{23} at short annealing times and at long annealing times this effect becomes insignificant (Fig. 11).

LONG-TERM CREEP BEHAVIOR

Effect of Crystallinity

To investigate the effect of crystallinity on creep behavior of PET films, a series of samples were prepared by annealing initially amorphous PET films for different periods of time in order to obtain samples which have random

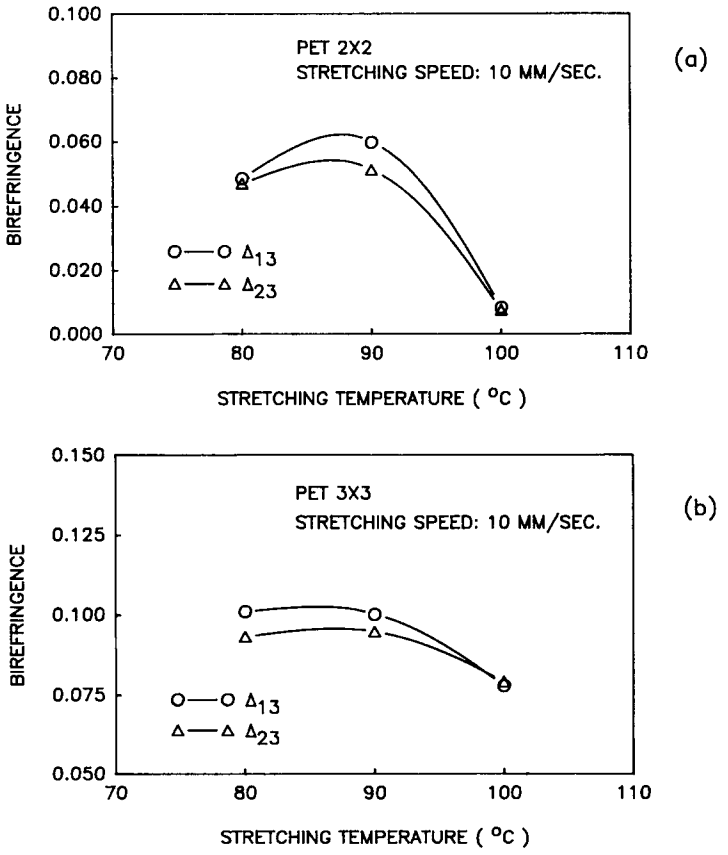

Fig. 10. Effect of stretching temperature on birefringences of (a) 2×2 and (b) 3×3 stretched films.

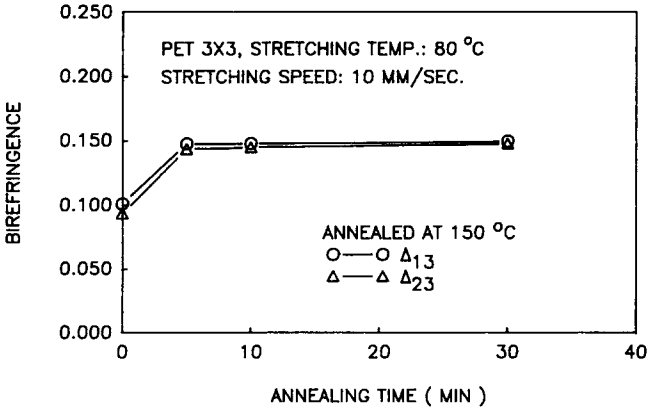

Fig. 11. Effect of annealing on birefringences of 3 × 3 stretched PET films.

chain orientation but different crystallinities. These samples were then subjected to tensile creep test. The creep behavior of these samples are presented in Figure 12. In these curves basically two creep regimes are noticeable. Short-term regime ($t < 10^4$ sec) followed by a long-term regime. At early creep times (up to 1000 sec) the differences in the creep strains are rather small and films with higher crystallinity exhibit lower creep strains. The main influence of crystallinity on the creep behavior becomes apparent at high creep times. The samples with higher crystallinities exhibit lower creep strains at all times. In addition, the increase of crystallinity drastically reduces the slope of the regime II which is situated beyond 1.10^4 sec.

Effect of Film Stretching Temperature

Stretching temperature is another important parameter affecting creep behavior of stretched PET samples since it influences both the chain orientation and level of crystallinity. As shown in Figure 13, PET films stretched at 80 and 90°C to 2 × 2 stretch ratio exhibit much lower creep strains especially at creep

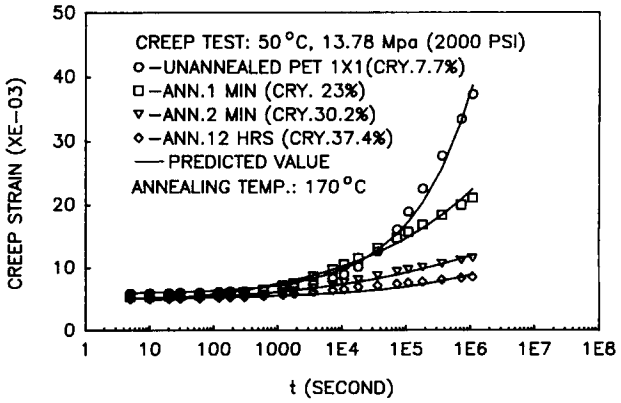

Fig. 12. Long-term creep behavior of unoriented PET films of different crystallinities.

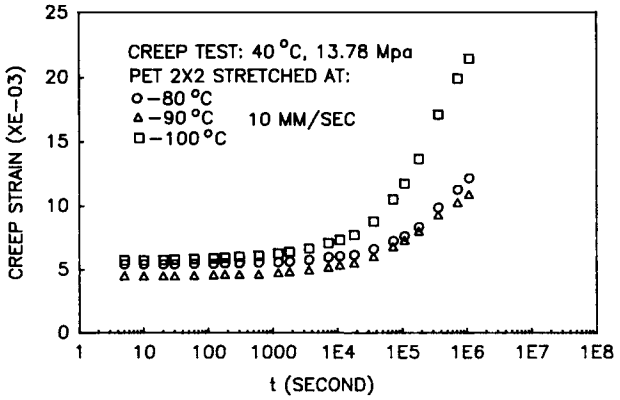

Fig. 13. Effect of film stretching temperature on the long-term creep behavior of 2 × 2 stretched films (testing temperature: 40°C).

times longer than 1.10^4 sec as compared to the film stretched at 100°C. This follows the trends observed in crystallinity and birefringences in these films (see Figs. 5 and 10). The films stretched to 3 × 3, on the other hand, show very small differences in creep curves obtained at 40°C testing temperature (Fig. 14a). The differences in creep curves of 3 × 3 stretched films become more pronounced when the creep testing is performed at 50°C [16°C below the glass transition temperature (Fig. 14b)] and follows the same trends as observed in 2 × 2 stretched films but the effect is relatively small.

Effect of Stretch Ratio

The effect of stretch ratio on creep behavior is demonstrated in Figures 15 and 16 for films stretched at 80°C and tested at 30°C under 6.89 MPA (1000 psi), 13.78 MPa (2000 psi) stress levels. The shape of these curves are all very similar to each other. Creep strains at times less than 1×10^4 sec are relatively constant and above this time appreciable deviations are observed. These two figures indicate that increasing the draw ratio drastically decreases the creep strain at all times and the lowest creep strain is observed in 3 × 3 stretched samples. Figures 15b and 16b show the creep strain rate as a function of strain for all three samples at 6.89 MPa (1000 psi) and 13.78 MPa (2000 psi) respectively. These figures indicate that the increase of stretch ratio results in a decrease of creep strain rate at any given strain. Creep strain rate levels off and shows a tendency to remain constant at high strain levels indicating steady-state creep at long creep times. This is typical of creep behavior of materials.[19,29] Similar results can be observed in Figures 17 and 18 in which the strains are plotted as a function of time and the creep strain rates are plotted as a function of strain for PET 1 × 1, 2 × 2 and 3 × 3 samples tested at 13.78 MPa (2000 psi) stress level and at 40°C and 50°C respectively. As expected the closer the testing temperatures to T_g, the higher the creep strains, and the effect of stretch ratio on the creep levels become more appreciable at higher temperatures. This is further demonstrated in Figures 19 and 20 where the effect of testing temperature on creep behavior of film stretched to 2 × 2 and 3 × 3 are presented.

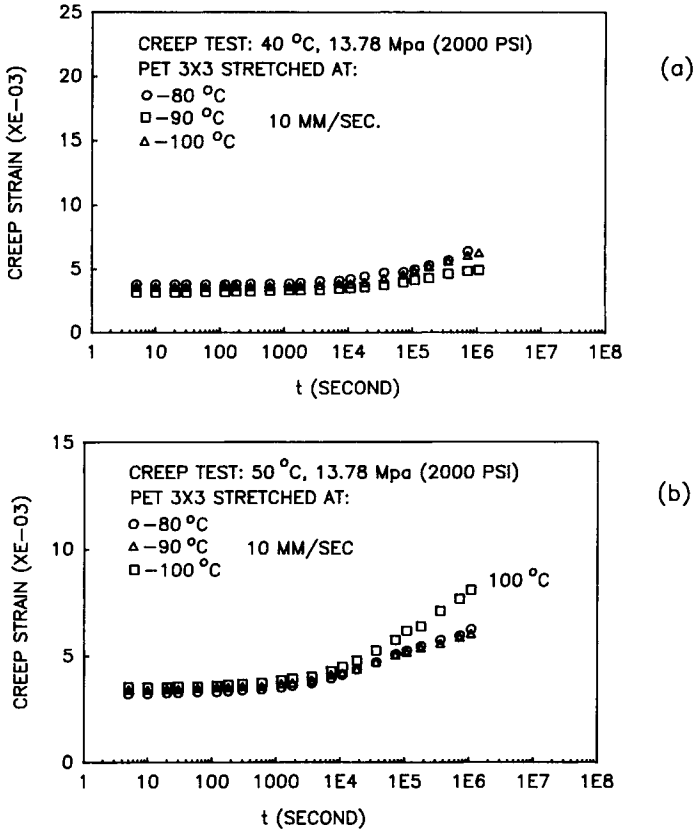

Fig. 14. Effect of film stretching temperature on the long-term creep behavior of 3 × 3 stretched films. [creep testing temperatures: (a) 40 and (b) 50°C].

These data indicate that the creep testing temperature has a pronounced effect on creep strain behavior at high creep times on films stretched to 2 × 2. However, this effect becomes almost negligible on films stretched to 3 × 3 stretch ratios as shown in Figure 20.

Effect of Annealing

Heat setting (annealing at elevated temperatures) after stretching of PET films is a common practice to enhance the dimensional stability of stretched films. This effect is demonstrated in Figure 21 for unstretched and 3 × 3 stretched films. In both cases creep strains decrease with annealing but the effect is more significant in unstretched films. This difference is attributed to high chain orientations and crystallinity levels in 3 × 3 stretched film and increase of crystallinity in initially amorphous and unoriented films is more substantial than in the stretched films. In unstretched films, the benefit of chain orientation on creep behavior is absent and only the crystallinity effects are observed.

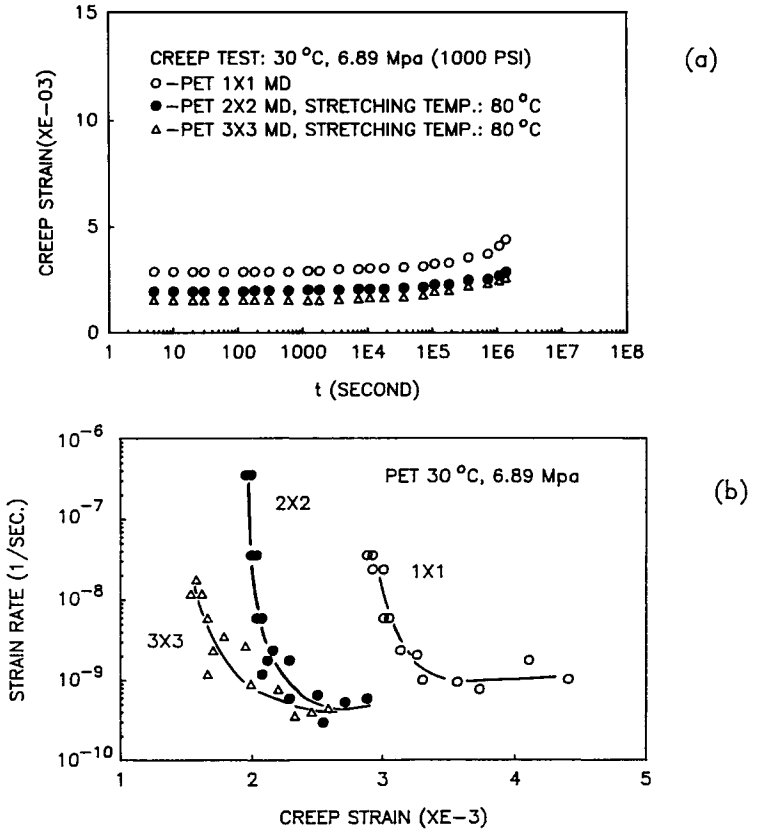

Fig. 15. The effect of stretch ratios on the creep behavior of unstretched and 2 × 2 and 3 × 3 stretched films. (process temperature: 80°C, test temperature: 30°C, stress: 6.89 MPa) (a) ϵ vs. $\log(t)$; (b) $\log(\epsilon')$ vs. ϵ.

In-Plane Anisotropy in Unbalanced Biaxially Stretched Films

In commercial processes such as tenter frame and tubular film blowing processes, balanced biaxial orientation is rarely attained, therefore, the films produced by these processes generally exhibit in-plane anisotropy. To investigate the anisotropy effects on the creep behavior of films we prepared films stretched to 3 × 1 and 3 × 2 stretch ratios at 80°C and tested the creep behavior in 0 (MD), 30, 60, and 90 (TD) directions in these films. As shown in Figures 22 and 23 creep strains are the lowest in the machine direction along which the highest deformation occurred in the films and the highest strains are observed in the transverse direction. The change of creep behavior between these two directions is not monotonous. There are large changes between 0, 30, and 60° directions but almost identical creep curves are obtained in 60 and 90° (TD) directions. This is also apparent in the polar representations of these data (Fig. 22b). In this figure, isochronous creep strains in different directions in the films plane are plotted. When the stretch ratio in TD is increased, the high in-plane anisotropy decreases as demonstrated in Figure 23a and b. In these figures an unexpected behavior is observed along the machine direction. As the trans-

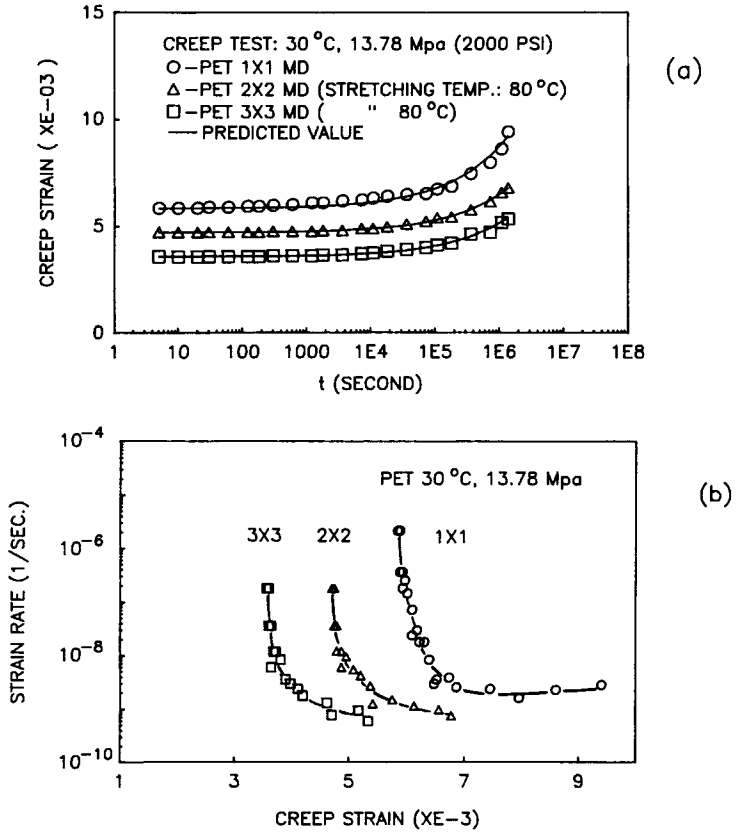

Fig. 16. The effect of stretch ratios on the creep behavior of unstretched and 2 × 2 and 3 × 3 stretched films. (process temperature: 80°C, test temperature: 30°C, stress: 13.78 MPa) (a) ϵ vs. $\log(t)$; (b) $\log(\epsilon')$ vs. ϵ.

verse stretch ratio increases, the creep strain in all directions except along MD decreases. In MD, this behavior is reversed. Note the crossover of lines in Figure 23c. This crossover is also observed in polar refractive index plots of these films. It appears that as the TD stretch ratio increases, the population of chains aligned along the MD decreases; this is reflected in the refractive index reduction and increase in creep strains. (See also Fig. 24 where creep curves only along MD are plotted for 3 × 1, 3 × 2, and 3 × 3 stretched films.)

Power Law Empirical Equation

The following empirical power law equation has been used to approximately predict creep strain of some polymers.[12,30,31]

$$e(t) = e_o + At^n\sigma^m\exp(-Q/RT) \tag{2}$$

where e_o is the elastic deformation, σ is the creep stress, Q is the activation energy, R is the gas constant, T is the absolute temperature, and A is a constant.

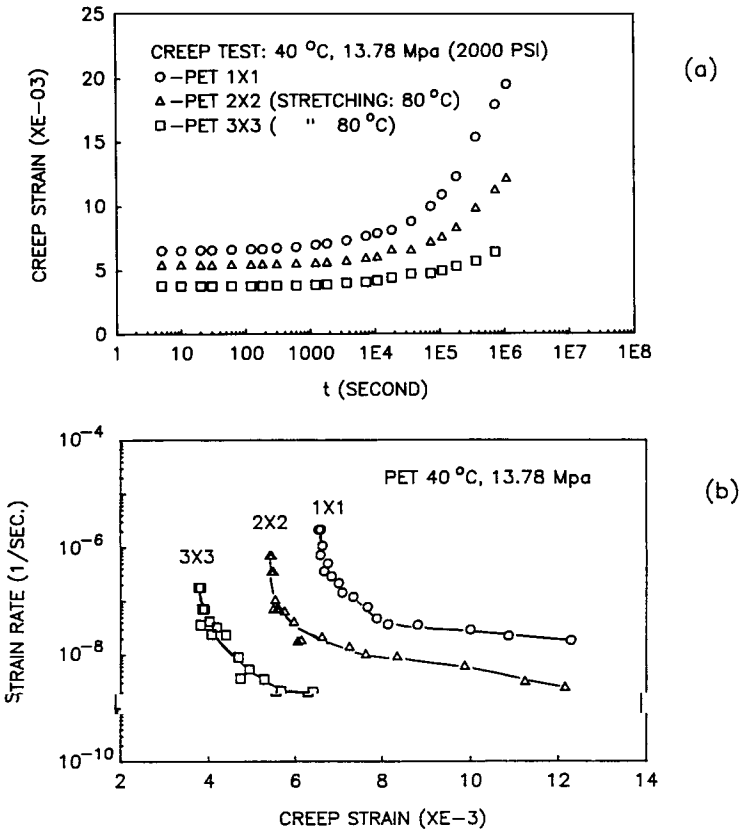

Fig. 17. The effect of stretch ratios on the creep behavior of unstretched and 2 × 2 and 3 × 3 stretched films. (process temperature: 80°C, test temperature: 40°C, stress: 13.78 MPa) (a) ϵ vs. $\log(t)$; (b) $\log(\epsilon')$ vs. ϵ.

In order to see whether this equation can be fitted to the experimental data of stretched PET films, eq. (2) is rewritten as

$$e(t) = e_o + at^n \tag{3}$$

where $a = A\sigma^m \exp(-Q/RT)$. For some samples, e_o, a and n values were determined using a least square curve fitting program and the values of e_o, a and n are listed in the Table III. The predicted creep strains for these samples are plotted in the previous figures as solid lines. From these figures it is clear that the power law equation fit reasonably well to the experimental data at creep times less than 10^6 sec.

Eq. (2) implies that A, n, and m should be constants for the same material tested at different conditions. In case of biaxially stretched PET films, the crystallinities and molecular orientation are different among the samples stretched to different stretch ratios and stretched at different conditions. Therefore, these constants may not keep the same values for all stretched samples. One possible way to investigate the effect of biaxial stretching on creep

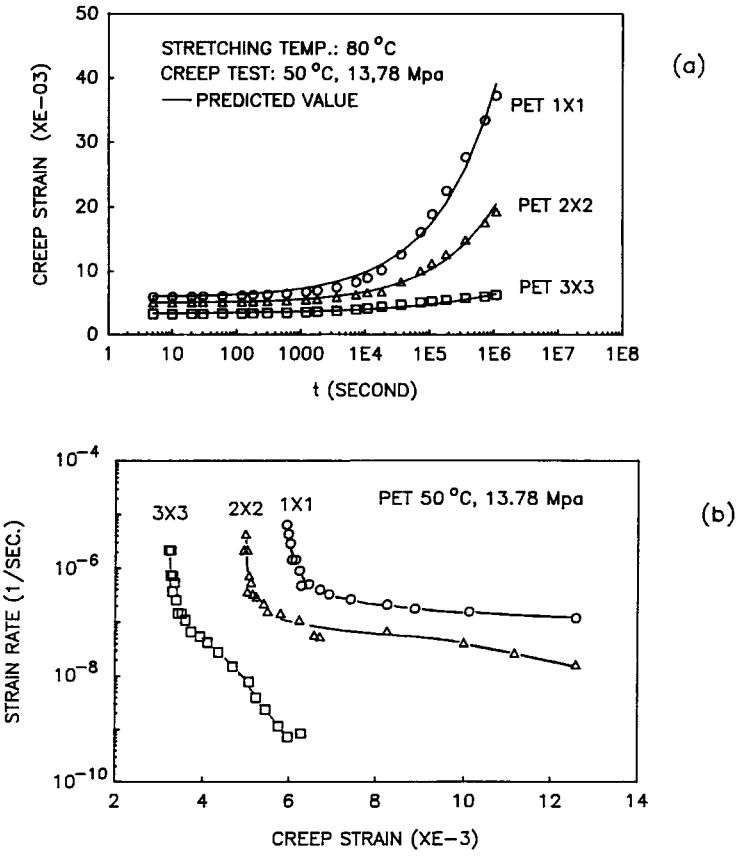

Fig. 18. The effect of stretch ratios on the creep behavior of unstretched and 2 × 2 and 3 × 3 stretched films. (process temperature: 80°C, test temperature: 50°C, stress: 13.78 MPa) (a) ϵ vs. $\log(t)$; (b) $\log(\epsilon')$ vs. ϵ.

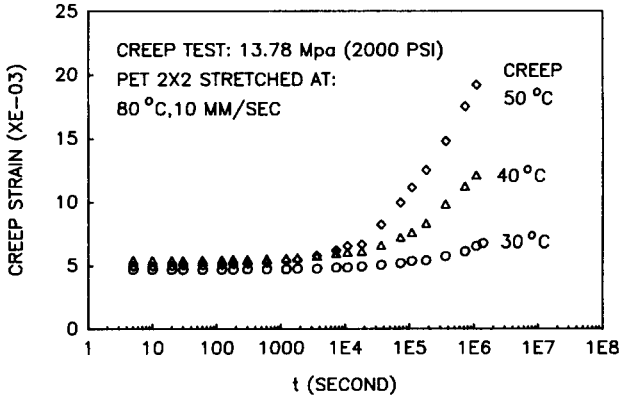

Fig. 19. Effect of creep testing temperature on long-term creep behavior of 2 × 2 stretched films (process temperature: 80°C, stress: 13.78).

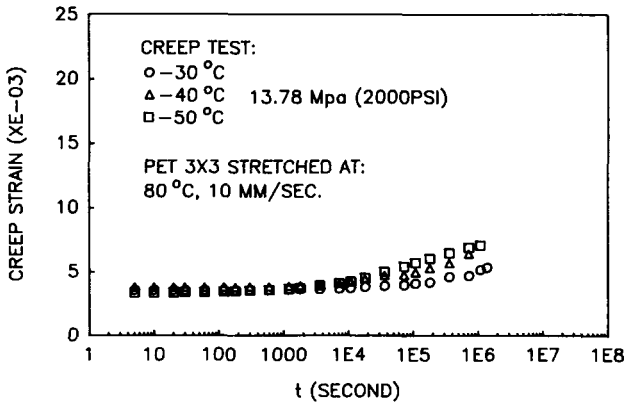

Fig. 20. Effect of creep testing temperature on long-term creep behavior of 3 × 3 stretched films (process temperature: 80°C, stress: 13.78).

behavior of PET is to see the changes of these parameters due to the different stretch ratios and different creep testing conditions. To do this the following procedures were used to determine all the parameters in eq. (2).

Again eq. (2) is rewritten as follows

$$e_c = e(t) - e_o = At^n\sigma^m \exp(-Q/RT) \tag{4}$$

where e_c is the pure creep strain, $e_o = \sigma/E$, and E is the elastic modulus. To determine activation energies (Q) of PET 1 × 1, 2 × 2, and 3 × 3 stretched at 80°C, ln e_c is plotted as a function of $1/T$ for constant creep time t = 72,000 sec and under stress σ = 6.89 and 20.67 MPa (1000 and 3000 psi) in Figure 25a and b respectively. Since ln $e_c = -Q/RT$ + constant, activation energies Q were calculated from the slopes of ln $e_c - 1/T$ straight lines that were fitted to experiment data for PET 1 × 1, 2 × 2, and 3 × 3 using the linear regression method. The calculated activation energies for stretched PET samples are plot-

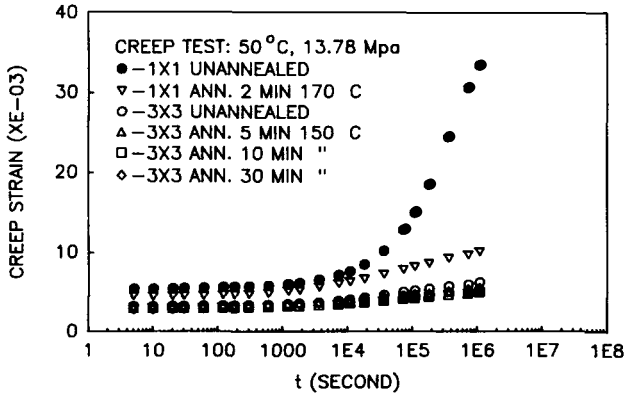

Fig. 21. Effect of heat setting on long-term creep behavior of unstretched and 3 × 3 stretched films (process temperature: 80°C, stress: 13.78 MPa).

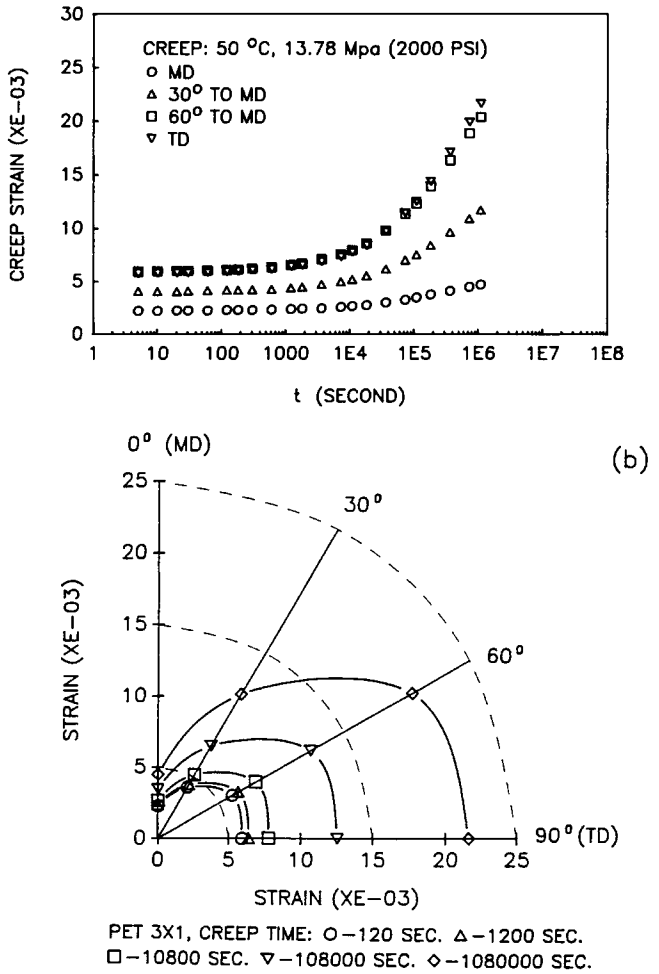

Fig. 22. (a) In-plane anisotropy in long-term creep behavior of 3 × 1 stretched films. (process temperature: 80°C, stress: 13.78 MPa); (b) Polar representation of the data in (a).

ted as a function of creep stresses in Figure 26. As expected, the increase of stretch ratio decreases the activation energies of PET films at any stress level. This indicates that highly stretched samples show lower creep strain dependence on temperature. That is, the increase of creep strain due to the temperature increase is smaller on highly stretched samples. Furthermore, all of the PET samples in Figure 25 show a similar tendency of increase of activation energy Q as stress increases.

Next, we keep the temperature constant and plot log e_c vs. log σ at a constant creep time. m Value in equation log e_c = m log σ + constant is the slope of log e_c − log σ curve. This is Figure 27a and b. m values for PET 1 × 1, 2 × 2, and 3 × 3 tested at 30, 40 (not shown), and 50°C were then determined from the slopes of these straight lines (Figure 27a and b). It is interesting to note that the samples stretched to different stretch ratios have almost the same m value at the same creep testing temperature. This suggests that biaxial stretching

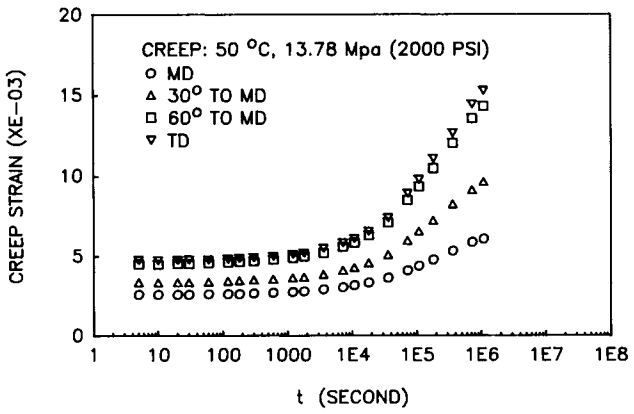

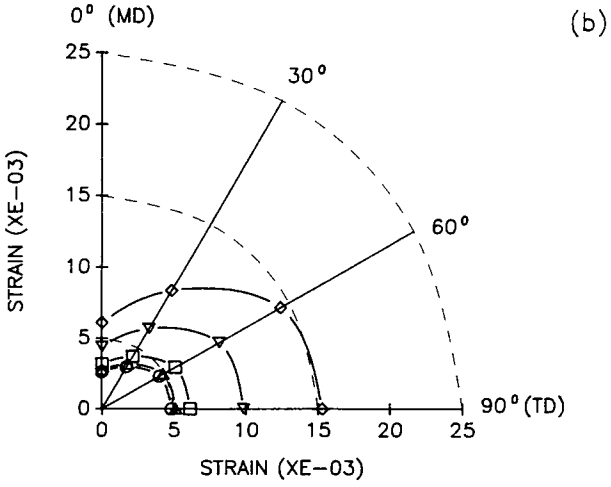

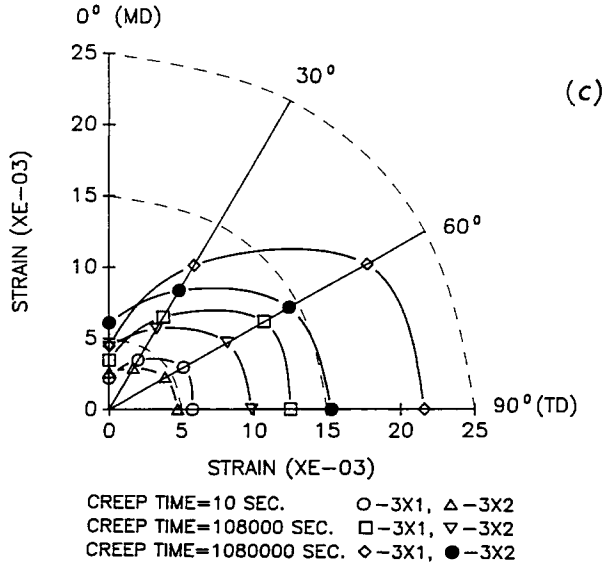

Fig. 23. (a) In-plane anisotropy in long-term creep behavior of 3 × 2 stretched films. (process temperature: 80°C, stress: 13.78 MPa); (b) polar representation of the data in (a); and (c) comparison of data in Figure 22a and Figure 23a in polar coordinates.

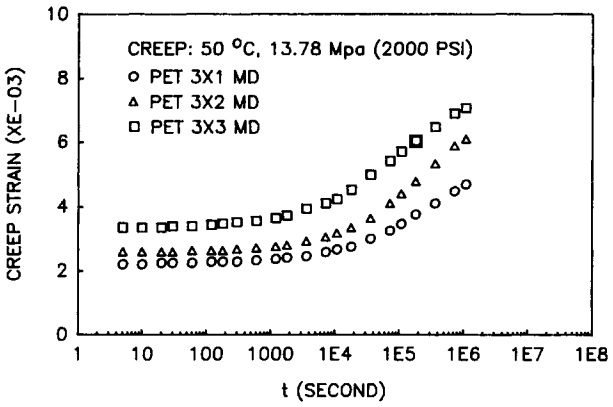

Fig. 24. Long-term creep behavior along the MD of 3 × 1, 3 × 2, and 3 × 3 stretched films. (process temperature: 80°C, stress: 13.78 MPa).

does not change the effect of stress on creep strain for PET films. The effect of increasing creep testing temperature is to increase m value as indicated in Figure 28 in which m values at each temperature are the average of the values of three different stretched samples. At lower temperatures, all PET samples show linear creep behavior under 6.89 to 20.67 MPa (1000 to 3000 psi) stress levels since m is close to 1.

Since the activation energy Q, m, and n values are known, the coefficient A in eq. (2) can be calculated based on "a" values in the Table III. Thus, the power law equations for as-received PET (1 × 1) and PET 3 × 3 stretched at 80°C and 10 mm/sec and tested at 50°C are listed below

$$e(t)_{(1\times1)} = 5.8893 \times 10^{-3} + 1.55 \times 10^{-11}\sigma^2 t^{0.4467}\exp(-0.0410)$$

$$e(t)_{(3\times3)} = 3.2167 \times 10^{-3} + 1.36 \times 10^{-11}\sigma^2 t^{0.2990}\exp(-0.0224)$$

TABLE III*

PET sample ID	e_o ($\times 10^{-3}$)	a ($\times 10^{-3}$)	n	Temperature (°C)
1 × 1 (as-received)	5.8420	0.002884	0.4970	30
2 × 2 80°C	4.6990	0.001974	0.4920	30
3 × 3 80°C	3.6660	0.001729	0.4910	30
1 × 1 (as-received)	6.5178	0.02630	0.4467	40
2 × 2 90°C	4.4830	0.02903	0.3911	40
3 × 3 90°C	3.1197	0.02640	0.3069	40
1 × 1 (as-received)	5.8893	0.05930	0.4557	50
2 × 2 80°C	4.9531	0.02640	0.4591	50
3 × 3 80°C	3.2167	0.05300	0.2990	50
1 × 1 ann. 55 sec 170°C	5.0000	0.8803	0.2779	50
1 × 1 ann. 1 min 170°C	3.3377	0.9112	0.2179	50
1 × 1 ann. 2 min 170°C	3.7060	0.7618	0.1724	50
1 × 1 ann. 12 h 170°C	4.5300	0.3700	0.1760	50

* Load 13.78 MPa (2000 psi), stretch speed: 10 mm/s.

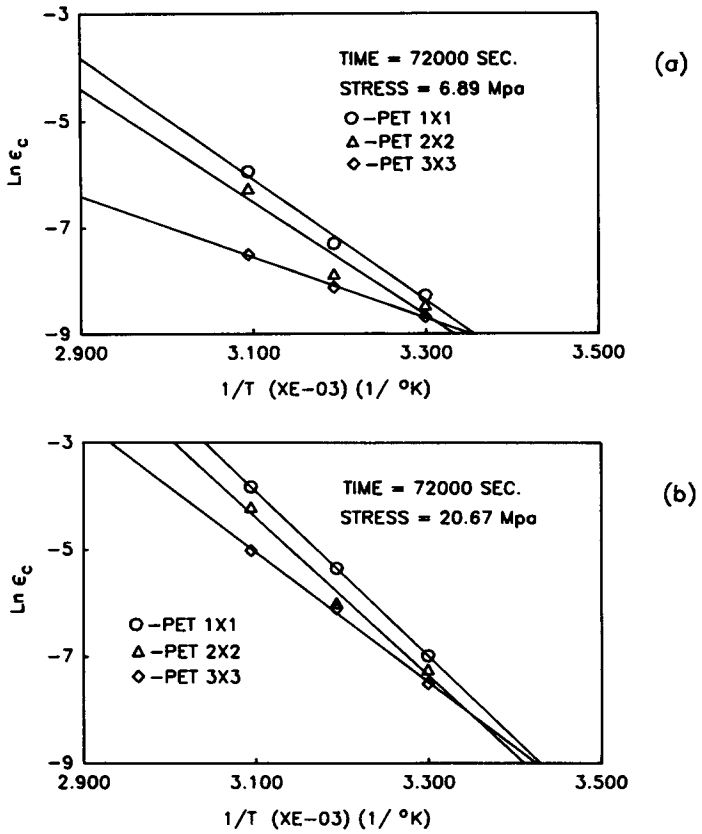

Fig. 25. log (e_c) vs. $1/T$ for unstretched, 2 × 2, and 3 × 3 stretched films at $t = 7.2.10^4$ sec. (a) 6.89 MPa; (b) 20.67 MPa.

where $e(t)$ is the creep strain, σ (psi), and t (sec). From these two strain representations it is evident that biaxial stretching decreases all the parameters in eq. (2) except for m which remain constant at testing temperature. Fur-

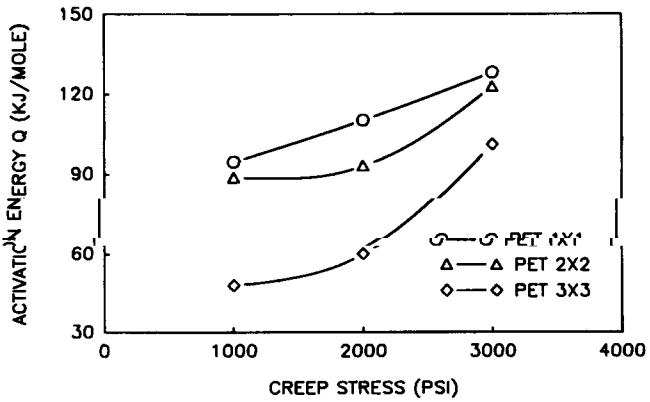

Fig. 26. Activation energy vs. creep stress.

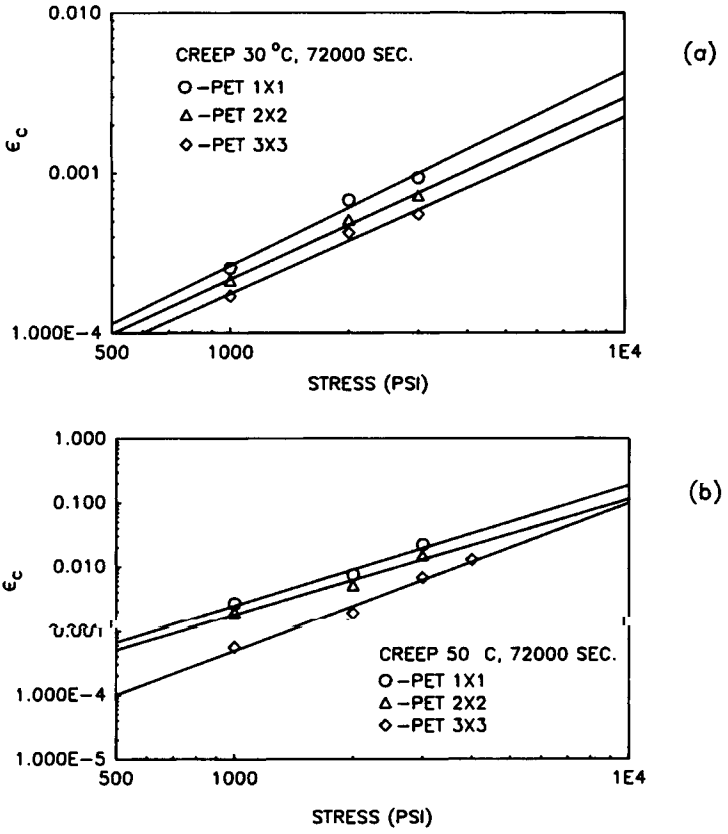

Fig. 27. log (e_c) vs. stress.

thermore, the Parameters A and n in the power law equation are the most important factors affecting creep strains of PET films. The smaller these parameters are, the lower the creep strain is. The parameters A and n may be

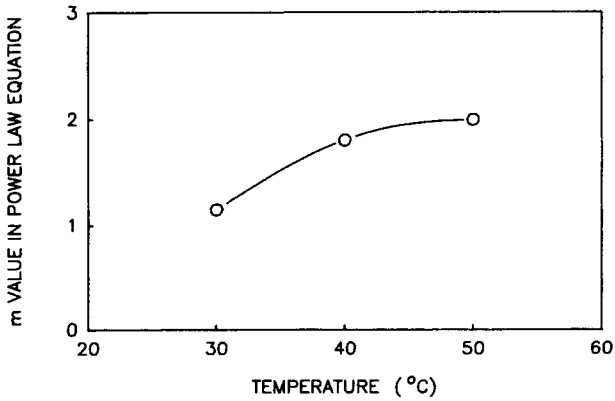

Fig. 28. m Vs. temperature.

functions of crystallinity and molecular orientation. The increases of crystallinity and molecular orientation induced by biaxial stretching results in the decreases of either A or n or both.

As mentioned earlier, the power law equation is satisfactory for predicting creep strains of PET films at the creep times less than 10^6 sec. After 10^6 sec, appreciable deviations appear. In addition, it is difficult to write a power law representation which can predict creep behavior of the stretched PET samples under any testing condition since the effect of stress on strain (m) and activation energy (Q) is not constant. m Value increases as the temperature increases while the activation energy Q increases acceleratively as stress increases.

CONCLUSIONS

We have demonstrated that key structural parameters: crystallinity, level, and type of orientation distribution imposed by the stretching process have significant influence on the tensile creep behavior and its anisotropy in PET films at temperatures below the glass transition temperature. Creep curves exhibited two characteristic regimes: one at short creep times ($< 1.10^4$ sec), the other at long creep times. Increase of crystallinity and increase of chain orientation in a given testing direction invariably causes a rapid reduction in creep strain values particularly at long creep times (regime II). Creep strain rate reaches constant values at high strain levels and these constant values are lower for films possessing higher crystallinity and/or orientation. It appears that the network structure formed by the crystalline regions significantly reduces the creep strains and strain rates by acting as anchor to various portions of chains by entrapping them in higher density/less mobile crystalline regions. Other than its positive influence, detailed physical explanation of effect of chain orientation on the creep behavior is more difficult since both orientation and crystallinity increase accompany each other during the processing making it difficult to isolate the purely orientational effects. Nevertheless, based on our experiments, we can conclude a few points. We saw that chain orientation and orientational anisotropy evidenced by the optical properties have significant effect on creep behavior. In particular, this was clearly noticed in unbalanced biaxially stretched films where TD stretching reduced the refractive index in MD (refractive index is highest along the chain axis in PET[28]) which, in turn, resulted in increase of creep strains in that direction. Simple reorientation of part of the population of chains towards TD caused increased creep strains in MD.

In our studies, power law type curve fitting was partially successful. However, the parameters in the power law representation are mostly dependent on the structural parameters and testing parameters. We have also tried a model consisting of Maxwell and Voigt elements in series[20] without success. It is clear that the presently available models to predict the creep behavior in products possessing complex orientation distribution and varying crystallinities are not satisfactory and more work is needed to improve the predictive capabilities of the presently available models or new models incorporating key structural parameters need to be developed.

We would like to thank Mr. Mark Dannis for his help in designing the creep chamber. This work was supported by the Department of Energy Solar Energy Research Institute (Subcontract No.: XK-6-05059-1). We also would like to thank Dr. Paul Schissel of the Solar Energy Research Institute for suggesting us to work on the creep behavior of biaxially stretched films.

References

1. O. D. Sherby and J. E. Dorn, *J. Mech. and Phys. of Solids,* **6,** 145 (1958).
2. N. Brown, B. D. Metzger, and Y. Imai, *J. Polym. Sci. Phys.,* **16,** 1085 (1978).
3. J. Smart and J. G. Williams, *J. Mech. Phys. of Solids,* **20,** 325 (1972).
4. D. G. O'Connor and W. N. Findley, *J. Eng. for Industry,* May, 237 (1962).
5. D. L. Questad, *Polym. Eng. Sci.,* **26,** 269 (1986).
6. J. E. Sinclair and L. J. Edgemond, *J. Appl. Polym. Sci.,* **13,** 999 (1969).
7. J. M. Crissman and L. J. Zappas, *Polym. Eng. Sci.,* **19,** 99 (1979).
8. L. J. Zappas and J. M. Crissman, *Polym. Eng. Sci.,* **19,** 104 (1979).
9. S. Turner, *Brit. Plast.,* Sept., 501 (1964).
10. N. G. McCrum, *J. Matl. Sci.,* **13,** 1596 (1978).
11. S. Turner, *Brit. Plast.,* August, 440 (1964).
12. G. G. Tantina, *Polym. Eng. Sci.,* **26**(11), 776 (1986).
13. I. M. Ward, *Polymer,* **5,** 59 (1964).
14. I. M. Ward and J. M. Wolf, *J. Mech. Phys. Solids* **14,** 131 (1966).
15. D. W. Hadley and I. M. Ward, *J. Mech. Phys. Solids,* **13,** 397 (1965).
16. M. W. Darlington and D. W. Saunders, *J. Macromol. Sci. Phys.,* **B5,** 207 (1971).
17. I. M. Ward and E. T. Onat, *J. Mech. Phys. Solids,* **11,** 217 (1963).
18. M. G. Brereton, S. G. Croll, R. A. Duckett, and I. M. Ward, *J. Mech. Phys. Solids,* **22,** 97 (1974).
19. C. J. Fost and I. M. Ward, *J. Mech. Phys. Solids,* **20,** 165 (1972).
20. M. A. Wilding and I. M. Ward, *Polymer,* **19,** 969 (1978).
21. G. Tittomanlio and G. Rizzo, *J. Appl. Polym. Sci.,* **21,** 2933 (1977).
22. J. Marin and P. B. Griesacker, *J. Appl. Polym. Sci.,* **7,** 134 (1963).
23. R. W. Appleby and W. Kenbusfield, *Polymer Commun.,* **27,** 45 (1986).
24. V. G. Yurkevich, V. L. Karpov, B. L. Zverev, and L. B. Alexandrova, *J. Polym. Sci. Polym. Symp.,* **42,** 859 (1973).
25. W. L. Wallach, *J. Polym. Sci.,* **C13,** 69 (1966).
26. R. J. Samuels, *J. Appl. Polym. Sci.,* **26,** 1383 (1981).
27. M. Cakmak, J. L. White, and J. E. Spruiell, (to be submitted).
28. M. Cakmak, J. L. White, and J. E. Spruiell, *Polym. Eng. Sci.* **29**(21), 1534 (1989).
29. W. D. Callister Jr., *Materials Science and Engineering,* Wiley, New York (1985).
30. W. N. Findley and D. B. Paterson, *Proc. ASTM,* **58,** 841 (1958).
31. W. N. Findley and J. F. Tracy, *Polym. Eng. Sci.,* **14,** 577 (1974).

Received April 28, 1989
Accepted December 13, 1989